J|A|C|S
ARTICLES
Published on Web 02/07/2002

Hydrogen and Higher Shell Contributions in Zn^{2+}, Ni^{2+}, and Co^{2+} Aqueous Solutions: An X-ray Absorption Fine Structure and Molecular Dynamics Study

Paola D'Angelo,*[,§,||] Vincenzo Barone,[‡] Giovanni Chillemi,[†] Nico Sanna,[†] Wolfram Meyer-Klaucke,[#] and Nicolae Viorel Pavel[§]

Contribution from the Dipartimento di Chimica, Università di Roma "La Sapienza", P. le A. Moro 5, 00185 Roma, Italy, Dipartimento di Chimica, Università di Napoli "Federico II", Complesso Universitario di Monte S. Angelo Via Cintia, 80126 NAPOLI, Italy, CASPUR, c/o Università di Roma "La Sapienza", P. le A. Moro 5, 00185 Roma, Italy, and EMBL Outstation Hamburg, c/o DESY, Notkestrasse 85, D-22603, Hamburg, Germany, INFM UdR CM, Dipartimento di Chimica, Universitá di Napoli "Federico II", Complesso Universitario di Monte S. Angelo Via Cintia, 80126 NAPOLI, Italy

Received February 17, 2001. Revised Manuscript Received November 9, 2001

Abstract: A detailed investigation of the hydration structure of Zn^{2+}, Ni^{2+}, and Co^{2+} in water solutions has been carried out combining X-ray absorption fine structure (EXAFS) spectroscopy and Molecular Dynamics (MD) simulations. The first quantitative analysis of EXAFS from hydrogen atoms in 3d transition metal ions in aqueous solutions has been carried out and the ion−hydrogen interactions have been found to provide a detectable contribution to the EXAFS spectra. An accurate determination of the structural parameters associated with the first hydration shell has been performed and compared with previous experimental results. No evidence of significant contributions from the second hydration shell to the EXAFS signal has been found for these solutions, while the inclusion of the hydrogen signal has been found to be important in performing a quantitative analysis of the experimental data. The high-frequency contribution present in the EXAFS spectra has been found to be due to multiple scattering (MS) effects inside the ion−oxygen first coordination shell. MD has been used to generate three-body distribution functions from which a reliable analysis of the MS contributions to the EXAFS spectra of these systems has been carried out.

1. Introduction

Nowadays it is well established that a thorough understanding of many chemical properties of ionic solutions should be based on the precise knowledge of their coordination geometry. An important and sometimes demanding task in this context is to determine the structure of aqua complexes of several metal ions. A large number of studies have been carried out and the structural properties of the first hydration shell for many metal ions are now understood reasonably well.[1−4] However, the situation is different concerning the coordination of water molecules in the second hydration shell. Information on the long distance range is much more difficult to gain even if neutron diffraction investigations have pointed out the presence of a weakly coordinated second shell in the case of Ni^{2+}, Fe^{2+}, Fe^{3+}, and Cr^{3+} aqueous solutions.[3]

During the past several years it has been shown that X-ray absorption spectroscopy (XAS) is particularly well suited for the investigation of the local solvent structure of ions dissolved in water, due to its atomic selectivity and its sensitivity to dilute solutions. Whereas pair distribution functions can also be obtained by diffraction techniques, the extended X-ray absorption fine structure (EXAFS) spectroscopy offers a unique opportunity to determine higher order correlation functions describing the ion−solvent associations that exist in solution. The presence of these functions appears in the XAS spectra as multiple scattering (MS) effects, and the importance of accounting for these contributions in ionic solutions has been pointed out in several papers.[5−7]

Recently, a number of articles have been devoted to EXAFS studies of hydration of 3d transition metal ions and there is controversy as to whether the second hydration shell of these aqua ions is observable by EXAFS.[8−13] It is well established

§ Università di Roma "La Sapienza".
‡ Università di Napoli "Federico II".
† CASPUR.
# EMBL Outstation Hamburg.
|| INFM UdR CM.

(1) Magini, M.; Licheri, G.; Paschina, G.; Piccaluga, G.; Pinna, G. *X-ray Diffraction of Ions in Aqueous Solutions: Hydration and Complex Formation*; CRC Press: Boca Raton, FL, 1988.
(2) Ohtaki, H.; Radnai, T. *Chem. Rev.* **1993**, *93*, 1157.
(3) Enderby, J. E. *Chem. Soc. Rev.* **1995**, *24*, 159.
(4) Marcus, Y. *Chem. Rev.* **1988**, *88*, 1475.
(5) Benfatto, M.; Natoli, C. R.; Bianconi, A.; García, J.; Marcelli, A.; Fanfoni, M.; Davoli, I. *Phys. Rev. B* **1986**, *34*, 5774.
(6) Filipponi, A.; D'Angelo, P.; Pavel, N. V.; Di Cicco, A. *Chem. Phys. Lett.* **1994**, *225*, 150.
(7) D'Angelo, P.; Pavel, N. V. *J. Chem. Phys.* **1999**, *111*, 5107.
(8) Muñoz-Páez, A.; Pappalardo, R. R.; Sánchez Marcos, E. *J. Am. Chem. Soc.* **1995**, *117*, 11710.
(9) Kuzmin, A.; Obst, S.; Purans, J. *J. Phys.: Condens. Matter* **1997**, *9*, 10065.
(10) Lindqvist-Reis, P.; Muñoz-Páez, A.; Díaz-Moreno, S.; Pattanaik, S.; Persson, I.; Sandström, M. *Inorg. Chem.* **1998**, *37*, 6675.

10.1021/ja015685x CCC: $22.00

that the inner hydration shell of Zn^{2+}, Ni^{2+}, and Co^{2+} has an octahedral structure with six tightly bound water molecules. In these systems the second shell consists of about 12−14 loosely bound water molecules at a distance close to twice that of the inner shell. The experimental EXAFS spectra of 3d transition metal ions in aqueous solutions show a dominant low-frequency signal associated with the water molecules in the first coordination shell, and a weak high-frequency component which has been attributed either to MS effects or to the second hydration shell. This is ambiguous because the single scattering (SS) signal associated with the second shell has the same frequency as some of the MS paths in the first shell.

All the EXAFS analyses on 3d transition metal aqueous complexes have been performed up to now by taking into account the oxygen shells around the ions only, and neglecting any contribution coming from the hydrogen atoms of the water molecules. The influence of hydrogen atoms in the XAS spectra is expected to be very weak due to the low scattering power of this species, and it has usually been neglected in the EXAFS data analysis. Nevertheless, some examples are reported in the literature where the presence of hydrogen atoms has been taken into account. The effect of hydrogens on the X-ray absorption near edge structure (XANES) and EXAFS spectra of solid Ni and Cr hydrides has been considered indirectly through the modification in magnitude and phase of the photoelectron wave.[14] The hydrogen contribution has been observed experimentally in the EXAFS spectra of gaseous HBr,[15] Sr^{2+},[16,17] Ba^{2+},[18] and Br^{-}[19] aqueous and nonaqueous solutions and it has been included in XANES theoretical calculations of Ni^{2+} and Co^{2+} complexes in water solutions.[20]

A limitation of the XAS technique that has to be mentioned is its low sensitivity to large distances, especially for solutions where the EXAFS oscillations are expected to be weak. Moreover, for disordered systems the pair distribution functions around the photoabsorber atom can be strongly asymmetric and the standard Gaussian approximation may produce significant errors even when an apparently reasonable fit to the experimental data is obtained.[19,21,22] To overcome this limitation we have performed the EXAFS data analysis of Zn^{2+}, Ni^{2+}, and Co^{2+} aqueous solutions starting from pair and three-body distribution functions obtained from molecular dynamics (MD) simulations.[23] This approach has been used in the past to investigate different ionic solutions providing an accurate description of the coordination structure around the ion.[7,16−19,21]

The aim of this work is to provide a definite answer to whether the second hydration shell in Zn^{2+}, Ni^{2+}, and Co^{2+} aqueous solutions is detectable by EXAFS, to show which contributions are responsible for the high-frequency signal present in the experimental data, and to assess the sensitivity of the XAS technique to the presence of hydrogen atoms.

2. Methods

2.1. EXAFS Measurements. Zn^{2+}, Ni^{2+} and Co^{2+} aqueous solutions (0.2 M) were obtained by dissolving the appropriate amount of $Zn(NO_3)_2$, $Ni(NO_3)_2$, and $Co(NO_3)_2$ in water, respectively. EXAFS spectra at the Zn, Ni, and Co K-edges were recorded in transmission mode with use of the EMBL spectrometer at DESY.[24] Measurements were performed at room temperature with a Si(111) double-crystal monochromator and 50% harmonic rejection achieved by slightly detuning the two crystals from parallel alignment.[25] For each sample three spectra were recorded and averaged after performing an absolute energy calibration.[25,26] The DORIS III storage ring was running at an energy of 4.4 GeV with positron currents between 70 and 40 mA. The solutions were kept in cells with Kapton film windows and Teflon spacers of 2 mm for Zn and 1 mm for Co and Ni.

2.2. Data Analysis. In the case of disordered systems, reliable structural information can be obtained from the EXAFS spectra only if care is taken in the data analysis. As previously mentioned, the application of Gaussian approximation in the description of the coordination shells around the photoabsorber can produce significant errors in the determination of the structural parameters.[27,28] Moreover, due to the short-range sensitivity of the XAS technique, reliable structural information is frequently restricted to the first-neighbor shell, only. A method to analyze EXAFS spectra of liquid systems combining long-range information on the pair distribution functions $g(r)$'s obtained from MD simulations with the short-range sensitivity of the EXAFS technique has been described in previous papers.[21,22] It has been shown that a thorough insight into the interpretation of the EXAFS from ionic solutions can be obtained on the whole distance range by refining MD $g(r)$ models on the basis of the EXAFS experimental data. In the present investigation molecular dynamics simulations were used to obtain $g(r)$ starting models for Zn^{2+}, Ni^{2+}, and Co^{2+} aqueous solutions. Simulations were performed by using the extended simple point charge (SPC/E) model[29] for water−water interactions and potential functions for Zn^{2+}−, Ni^{2+}−, and Co^{2+}−water interactions were developed as part of this study. All details on the potential generation and MD simulations can be found in ref 23. Figure 1 shows the Zn^{2+}, Ni^{2+}, and Co^{2+} ion−water radial distribution functions and the corresponding running integration numbers obtained from MD calculations.[23] The ion−O and ion−H $g(r)$'s show very sharp and well-separated first peaks indicating the presence of a well-organized nearest-neighbor hydration shell. Note that the ion−H $g(r)$ first peaks fall in a region where no ion−O contacts are present. This indicates the existence of a preferential orientation of the water molecules in the first solvation shell, as confirmed by the probability density of the tilt angles shown in ref 23. In all cases, the integration over the ion−O first peak gives a coordination number of six in agreement with the existence of an octahedral structure around the ions. The number of water molecules in the second hydration shell, which is not easily accessible for experiments, may be estimated from the simulations. For all three systems the MD ion−O $g(r)$ second peaks indicate the existence of well-defined second hydration shells containing about twice the number of molecules of the first shell.

To extract structural information from the EXAFS data, we used an advanced scheme based on a multiple scattering formalism. The relation between the EXAFS $\chi(k)$ signal and the local structure, defined through the n-body distribution functions, contains the integrals of the two-

(11) Sakane, H.; Muñoz-Páez, A.; Díaz-Moreno, S.; Martinez, J. M.; Pappalardo, R. R.; Sánchez Marcos, E. *J. Am. Chem. Soc.* **1998**, *120*, 10397.
(12) Campbell, L.; Rehr, J. J.; Schenter, G. K.; McCarthy, M. I.; Dixon, D. *J. Synchrotron. Rad.* **1999**, *6*, 310.
(13) Read, M. C.; Sandström, M. *Acta Chem. Scand.* **1992**, *46*, 1177.
(14) Lengeler, B. *Phys. Rev. Lett.* **1984**, *53*, 74.
(15) D'Angelo, P.; Di Cicco, A.; Filipponi, A.; Pavel, N. V. *Phys. Rev. A* **1993**, *47*, 2055.
(16) D'Angelo, P.; Nolting, H.-F.; Pavel, N. V. *Phys. Rev. A* **1996**, *53*, 798.
(17) Roccatano, D.; Berendsen, H. J. C.; D'Angelo, P. *J. Chem. Phys.* **1998**, *108*, 9487.
(18) D'Angelo, P.; Pavel, N. V.; Roccatano, D.; Nolting, H.-F. *Phys. Rev. B* **1996**, *54*, 12129.
(19) D'Angelo, P.; Di Nola, A.; Mangoni, M.; Pavel, N. V. *J. Chem. Phys.* **1996**, *104*, 1779.
(20) Benfatto, M.; Solera J. A.; Chaboy, J.; Proietti M. G.; García, J. *Phys. Rev. B* **1997**, *56*, 3447.
(21) D'Angelo, P.; Di Nola, A.; Filipponi, A.; Pavel, N. V.; Roccatano, D. *J. Chem. Phys.* **1994**, *100*, 985.
(22) Filipponi, A. *J. Phys.: Condens. Matter* **1994**, *6*, 8415.
(23) Chillemi, G.; D'Angelo, P.; Pavel, N. V.; Sanna, N.; Barone, V. *J. Am. Chem. Soc.* **2002**, *124*, 1968−1976.
(24) Hermes, C.; Gilberg, E.; Koch, M. H. *Nucl. Instrum. Methods Phys. Res.* **1984**, *222*, 207.
(25) Pettifer, R. F.; Hermes, C. *J. Phys. Colloq.* **1986**, *C8*, 127.
(26) Pettifer, R. F.; Hermes, C. *J. Appl. Crystallogr.* **1985**, *18*, 404.
(27) Crozier, D. E.; Rehr, J. J.; Ingalls, R. *X-ray Absorption: Principles, Applications, Tecniques of EXAFS, SEXAFS and XANES*; Koningsberger, D. C., Prins, R., Eds.; Wiley: New York, 1988; Chapter 9.
(28) Crozier, D. E. *Physica B* **1995**, *208* & *209*, 330.
(29) Berendsen, H. J. C.; Grigera, J. R.; Straatsma, T. P. *J. Phys. Chem.* **1987**, *91*, 6269.

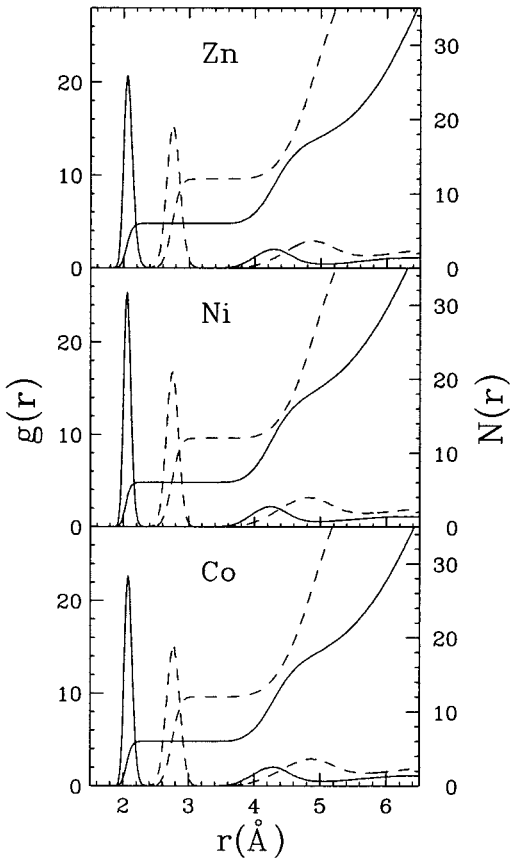

Figure 1. Ion−oxygen (full line) and ion−hydrogen (dashed line) pair distribution functions as derived from MD simulations for Zn^{2+}, Ni^{2+}, and Co^{2+} aqueous solutions (left scale) and corresponding running integration numbers (right scale).

atom ($\gamma^{(2)}$), three-atom ($\gamma^{(3)}$), and *n*-atom signals which can be calculated with use of the MS theory.[30]

In this work the ion−O and ion−H two-body $\chi(k)$ theoretical signals associated with the water molecules have been calculated starting from the pair distribution functions obtained from the MD simulations. Initial asymmetric peaks accounting for the first coordination shell around the photoabsorber have been obtained by splitting the ion−O and ion−H MD $g(r)$'s into an asymmetric peak and a second shell tail. As previously described,[21,22] these peaks are modeled with Γ-like distribution functions which depend on four parameters, namely the coordination number N, the average distance R, the mean-square variation σ, and the skewness β. Note that β is related to the third cumulant C_3 through the relation $C_3 = \sigma^3\beta$, and R is the first moment of the function $4\pi\int g(r)r^2\,dr$. It is important to stress that R is the average distance and not the position of the maximum of the peak (R_m). R is longer than R_m for asymmetric distributions while these values are equal for peaks which result in Gaussian functions ($\beta = 0$). The same fitting procedure has been applied to the ion−O $g(r)$ tails to gain information on the coordination structure of the second hydration shells. The MD parameters describing the ion−O $g(r)$ first and second peaks and the ion−H $g(r)$ first peaks are listed in Table 1. Note that the second shell peaks have been integrated up to 5 Å.

The $\chi(k)$ signals associated with the ion−O and the ion−H SS first shell distributions have been calculated by means of the GNXAS program,[30−32] and the initial MD asymmetric peak parameters have been optimized by fitting the EXAFS theoretical signal to the experimental data.

A different approach has been used to calculate the SS contribution associated with the second hydration shell. The short-range sensitivity of the EXAFS technique hampers the conclusive determination of the second hydration shell structure of ionic solutions. Therefore, the aid of structural information from other sources can be essential to perform a correct interpretation of the EXAFS data. For broad and asymmetric distribution of atoms, the $\chi(k)$ signal has to be represented by the equation:

$$\chi(k) = \int_0^\infty dr\, 4\pi\rho r^2 g(r) A(k,r) \sin[2kr + \phi(k,r)] \qquad (1)$$

where $A(k,r)$ and $\phi(k,r)$ are the amplitude and phase functions, respectively, and ρ is the density of the scattering atoms. The SS signals associated with the second hydration shells have been calculated by introducing into eq 1 the ion−O MD $g(r)$ tails obtained after subtraction of the first shell peak. This procedure allows one to perform the EXAFS analysis starting from reliable models for the first hydration shell and including the effective contribution of the second shells.

The analysis of the MS contributions has been carried out on the basis of the $g(r_1,r_2,\theta)$ distributions obtained from MD calculations. A detailed description of the three-dimensional arrangement of the water molecules around the Zn^{2+}, Ni^{2+}, and Co^{2+} ions is reported in ref 23. The orientation of water molecules in the first and second coordination shells has been obtained from the analysis of the O−ion−O and ion−$O_{1^{st}\,shell}$−$O_{2^{nd}\,shell}$ triangular configurations. In all cases the O−ion−O distributions show well-defined peaks at $\theta \simeq 90°$ and 180° in agreement with the expected octahedral coordination of these ions. The ion−$O_{1^{st}\,shell}$−$O_{2^{nd}\,shell}$ three-body distribution curves obtained from MD simulations are similar for the three ions and show a peak at an oxygen−oxygen distance of 2.75 Å, with a maximum located at $\theta \simeq 125°$. These are Gaussian-like distributions with $\sigma_\theta \simeq 13°$. About 17, 19, and 18 triangular configurations contribute to these peaks for Zn^{2+}, Ni^{2+}, and Co^{2+}, respectively, when an $O_{1^{st}\,shell}$−$O_{2^{nd}\,shell}$ cutoff distance of 5 Å is used. Note that a variation of 0.2 Å of the cutoff distance increases by one unit the number of configurations. The full set of parameters associated with the $g(r_1,r_2,\theta)$ distributions obtained from the MD simulations can be found in Table 6 of ref 23. From this analysis the distance−angle and the distance−distance correlations have been found to be negligible. The $\gamma^{(3)}$ signals associated with all the MD three-body distributions have been calculated by means of the GNXAS program and a thorough description of the theoretical framework for the multiple scattering analysis can be found in ref 30. Note that the knowledge of the thermal damping gained from the MD modeling can be used to determine the relative importance of MS signals. This method is extremely useful when diverse low-amplitude signals compete to form the EXAFS spectrum and there are too many parameters for the spectrum to be amenable to reliable fitting. The strongest MS contributions within the first hydration shell are generated by the three linear O−ion−O configurations. This is due to the focusing effect which enhances the amplitude of the three-body signals associated with linear configurations. Nevertheless, the MS signals associated with the twelve rectangular O−ion−O triangles provide a detectable contribution. The $\gamma^{(3)}$ signals associated with the ion−$O_{1^{st}\,shell}$−$O_{2^{nd}\,shell}$ three-body distributions have been calculated starting from the parameters obtained from MD simulations, and they have been found to be of negligible

Table 1. Structural Parameters for Zn^{2+}, Ni^{2+}, and Co^{2+} Water Solutions Obtained from the MD Simulations

		N	R (Å)	R_m (Å)	σ^2 (Å^2)	β
Zn−O	1st shell	6.0	2.08	2.07	0.0048	0.4
	2nd shell	12.2	4.40	4.27	0.11	0.5
Zn−H	1st shell	12.1	2.76	2.76	0.010	0.1
Ni−O	1st shell	6.0	2.07	2.06	0.0032	0.3
	2nd shell	13.4	4.39	4.27	0.12	0.6
Ni−H	1st shell	12.1	2.76	2.76	0.009	0.0
Co−O	1st shell	6.0	2.09	2.08	0.0038	0.3
	2nd shell	12.7	4.40	4.29	0.12	0.5
Co−H	1st shell	12.1	2.78	2.78	0.010	0.0

(30) Filipponi, A.; Di Cicco, A.; Natoli, C. R. *Phys. Rev. B* **1995**, *52*, 15122.
(31) Filipponi, A.; Di Cicco, A. *Phys. Rev. B* **1995**, *52*, 15135.

Table 2. Double-Electron Excitation Edge Parameters Obtained from the Fitting Procedures and Comparison with the $Z + 1$ Predictions[a]

		$E_d - E_t$	H	ΔE	E_{Z+1}
Zn	1s3p	105	0.11	26	103
	1s3s	164	0.02	42	160
Ni	1s3p	69	0.05	20	75−77
	1s3s	125	0.02	35	122
Co	1s3p	60	0.05	15	66−68
	1s3s	117	0.03	45	111

[a] The double-excitation energy onset E_d is measured from the first inflection point E_t. The absorption discontinuities H are given in K-edge jump units and the energies and the double-electron channel width parameters ΔE are given in eV.

amplitude. This result is in agreement with previous EXAFS investigations on Zn^{2+} water solutions where the Zn−$O_{1^{st}\,shell}$−$O_{2^{nd}\,shell}$ MS contribution was detectable only in the k-region below 4 Å^{-1} with an amplitude of about 1% of the total $\chi(k)$ signal.[9] The contributions of the MS processes, including the hydrogen atoms as scatterers, have as expected been found to be negligible due to the low scattering power of hydrogens.

Phase shifts have been calculated starting from one of the MD configurations of each ion, by using muffin-tin potentials and advanced models for the exchange-correlation self-energy (Hedin−Lundqvist).[33] The values of the muffin-tin radii are 0.2 and 0.9 Å, for hydrogen and oxygen, respectively, and 1.2 Å for zinc, nickel, and cobalt. The muffin-tin radius of the hydrogen atoms has been adjusted so as not to overestimate the signal from the scattering of hydrogen atoms, which is expected to be weak. The hydrogen muffin-tin radius chosen corresponds to about 0.06 electrons for the integral of the charge density. It has been verified that different MD configurations gave the same result. Inelastic losses of the photoelectron in the final state have been accounted for intrinsically by complex potential. The imaginary part also includes a constant factor accounting for the core-hole width (1.67, 1.44, and 1.33 eV for Zn, Ni, and Co, respectively).[34]

The data analysis of the raw spectra above the Zn, Ni, and Co K-edges was carried out by minimizing a residual function of the type:

$$R_i(\{\lambda\}) = \sum_{i=1}^{N} \frac{[\alpha_{exp}(E_i) - \alpha_{mod}(E_i; \lambda_1, \lambda_2, ..., \lambda_p)]^2}{\sigma_i^2} \qquad (2)$$

where N is the number of experimental points E_i, $\{\lambda\} = (\lambda_1, \lambda_2, ..., \lambda_p)$ are the p parameters to be refined, and σ_i^2 is the variance associated with each experimental point $\alpha_{exp}(E_i)$. In most cases σ_i^2 can be directly estimated from the experimental spectrum and a k^m weighting (with $m = 2, 3, ...$) results in a good approximation.[31,35]

It is well-known that the atomic backgrounds of several elements contain important contributions associated with the opening of multi-electron excitation channels. Here the background functions used to extract the $\chi(k)$ experimental signals have been modeled by means of step-shaped functions accounting for the 1s3p and 1s3s double-electron resonances. The energy onsets and the intensities of these channels are in agreement with previous determinations[36] and are listed in Table 2. A typical refinement of the Zn, Ni, and Co K-edge EXAFS spectra was performed by using the following structural parameters: the ion−O and ion−H first shell average distance R, variance σ^2, skewness β, and coordination number N; the angle θ, angle variance σ_θ^2, bond−bond $\rho_{R_1R_2}$ and bond−angle $\rho_{R_1\theta}$ dimensionless correlations for each 90° configuration; the angle variance σ_θ^2 and bond−bond $\rho_{R_1R_2}$ correlation for each 180° configuration. Note that the bond−bond $\rho_{R_1R_2}$ and bond−angle $\rho_{R_1\theta}$ correlation parameters are defined as $\rho_{R_1R_2} = \sigma^2_{R_1R_2}/\sqrt{\sigma^2_{R_1}\,\sigma^2_{R_2}}$ and $\rho_{R_1\theta} = \sigma^2_{R_1\theta}/\sqrt{\sigma^2_{R_1}\,\sigma^2_{\theta}}$ where $\sigma^2_{R_1R_2}$ and $\sigma^2_{R_1\theta}$ express the correlation between bond−bond and bond−angle vibration. The 180° angles were kept fixed at their equilibrium extremal values. Details about this parametrization of the three-body configurations can be found in ref 31. Other important nonstructural parameters included in the refinement were the energy difference between the experimental and theoretical scale and the amplitude correction factor S_0^2.

3. Results and Discussion

The XAFS analysis of the Zn^{2+}, Ni^{2+}, and Co^{2+} water solutions has been carried out starting from the structural parameters obtained from the MD simulations. Least-squares fits of the Zn^{2+} and Ni^{2+} experimental spectra have been performed in the range $k = 2.0-16.5$ Å^{-1}, while a smaller k-interval ($k = 2.1-15.2$ Å^{-1}) has been analyzed in the case of Co^{2+}. The spectra contained 880, 900, and 850 experimental points for Zn, Ni, and Co, respectively. Fitting procedures were applied to the whole set of structural and nonstructural parameters mentioned above to improve, as far as possible, the agreement between the calculated signals and the experimental spectra. The best-fit analyses of the Zn^{2+}, Ni^{2+}, and Co^{2+} water solution EXAFS spectra are shown in the upper panels of Figure 2. The $\gamma^{(n)}$ signals are shown multiplied by k^2 in Figure 2 and in the other figures throughout the paper, for better visualization. The first five curves from the top of each panel are the ion−O and ion−H first shell $\gamma^{(2)}$ contributions, the ion−O second shell signals, and the MS signals associated with the 3 linear and 12 orthogonal O−ion−O configurations. The reminder of the figures show the total theoretical contributions compared with the experimental spectra and the resulting residuals. Overall, the fitted EXAFS spectra match the experimental data quite well and the low-k behavior of the residual curves is most probably due to inaccuracies of the phase shift calculations. The R_i values obtained from the minimization procedures were 0.651×10^{-8}, 0.367×10^{-7}, and 0.230×10^{-7} for Zn, Ni, and Co, respectively. As expected, the dominant contribution to the total XAFS signal is given by the ion−O first shell signals, due also to the relatively large disorder that reduces the amplitude of the second-shell and MS contributions. As a consequence, the EXAFS structural refinement is particularly accurate for the shape of the ion−O $g(r)$'s first peaks. When looking at the $\chi(k)$ experimental spectra of Zn^{2+}, Ni^{2+}, and Co^{2+} aqueous solutions in Figure 2, it can be seen that the amplitude of the signal of the Zn^{2+} solution is the smallest, while the Ni^{2+} one is the largest.

The outstanding result of this analysis concerns the strong amplitude of the ion−H contributions. Due to the well-ordered structure of the water molecules around the ions, the 12 hydrogen atoms of the first hydration shell give rise to rather strong $\gamma^{(2)}$ signals, which are detectable up to about $k = 10$ Å^{-1}. The contribution of the second hydration shell is very small and the amplitudes of these signals are below the experimental noise of the spectra. On the contrary, the MS paths from O−ion−O linear and rectangular configurations yield higher amplitude signals in the low-k regions of the spectra.

The Fourier transform (FT) moduli of the EXAFS $\chi(k)k^2$ theoretical, experimental, and residual signals of the Zn^{2+}, Ni^{2+}, and Co^{2+} aqueous solutions are shown in the lower panels of Figure 2. The FT's have been calculated in the k-range 2.1−

(32) Filipponi, A. *J. Phys.: Condens. Matter* **1995**, *7*, 9343.
(33) Hedin, L.; Lundqvist, B. I. *J. Phys. C* **1971**, *4*, 2064.
(34) Krause, M. O.; Oliver, J. H. *J. Phys. Chem. Ref. Data* **1979**, *8*, 329.
(35) Burattini, E.; D'Angelo, P.; Di Cicco, A.; Filipponi, A.; Pavel, N. V. *J. Phys. Chem.* **1993**, *97*, 5486.
(36) Mihelič, A.; Padežnik Gomilšek J.; Kodre, A.; Arčon, I. *HASYLAB Annual Report 2000*, 209.

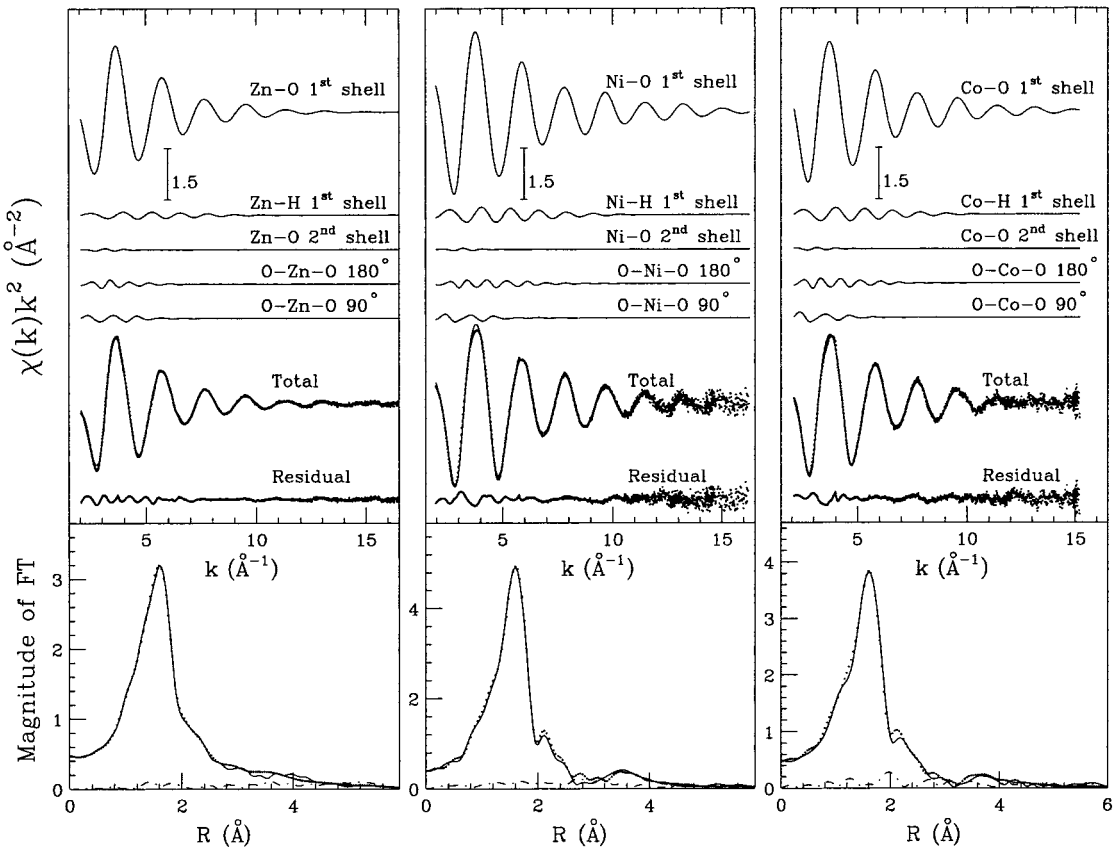

Figure 2. Fit of the 0.2 M Zn^{2+}, Ni^{2+}, and Co^{2+} water solutions (left, middle, and right upper panel, respectively). From the top to the bottom of each panel, the following curves are reported: the ion−O first shell signal, the ion−H first shell signal, the ion−O second shell signal, the O−ion−O linear and orthogonal three-body signals, the total theoretical signal compared with the experimental spectrum, and the residual curve. The lower panels show the nonphase-shift-corrected Fourier transforms of the experimental data (dotted line), of the total theoretical signals (full line), and of the residual curves (dashed−dotted line).

Table 3. First Shell Structural Parameters for Zn^{2+}, Ni^{2+}, and Co^{2+} Water Solutions Obtained from the EXAFS Data Analysis

	N	R (Å)	σ^2 (Å^2)	β
Zn−O	6.0(0.1)	2.078(0.002)	0.0087(0.0005)	0.2(0.1)
Zn−H	11.9(0.2)	2.78(0.02)	0.016(0.004)	0.04(0.09)
Ni−O	6.1(0.1)	2.072(0.003)	0.0046(0.0005)	0.5(0.2)
Ni−H	12.1(0.2)	2.77(0.02)	0.009(0.004)	0.03(0.05)
Co−O	6.0(0.1)	2.092(0.002)	0.0062(0.005)	0.3(0.1)
Co−H	12.1(0.2)	2.78(0.02)	0.010(0.004)	0.05(0.09)

13.5 Å^{-1} with no phase shift correction applied. The FT spectra show a prominent first shell peak that is mainly due to the ion−O first shell distance. Nevertheless, the ion−H FT peaks are located at 2.4 Å, giving rise to a shoulder on the first peak, which is more pronounced in the case of Ni and Co. A second peak is present in the FT spectra at about 3.8 Å. This is due to the MS paths within the first hydration shell even if the ion−O SS signal partially contributes to this peak. The accuracy and reliability of the present data analyses can be appreciated by looking at the agreement between the FT's of the theoretical and experimental signals.

Refined values for the full set of parameters defining the short-range peaks of the ion−O and ion−H $g(r)$'s are listed in Table 3. Note that the β values obtained for the three samples are very low (the largest β value in Table 3 is 0.5, which corresponds to a third cumulant of about 1.5×10^{-4}) and the resulting distributions are practically Gaussian in form. Statistical errors on structural parameters have been estimated by looking at the confidence intervals in the parameters' space. Standard deviations and correlation effects have been obtained from correlation maps calculated for the parameters of each shell. The estimated statistical errors associated with the 95% confidence interval have been obtained as described elsewhere.[31,32] The amplitude reduction factors S_0^2 were found to be 0.99 for all the three ions. In addition, the zero positions of the theoretical scales were found at 1.6 ± 0.5, 1.0 ± 0.5, and 1.4 ± 0.5 eV above the first inflection point of the spectra, for Zn, Ni, and Co, respectively.

As previously mentioned, the dominant contributions to the total EXAFS curves are made by the first-neighbor two-body signals, as shown in Figure 2. Even if the fitting procedures have been applied to the whole set of structural parameters mentioned above, only the ion−O and ion−H first neighbor structural parameters can be accurately refined, due to the weak amplitude of the MS signals. Therefore, information on $g(r_1,r_2,\theta)$ distributions obtained from MD simulations is essential to perform a reliable analysis of the MS effects associated with the first hydration shells. Note that according to the parametrization of the three-body distributions used in the GNXAS code the ion−O distance and σ^2 values are constrained by the first shell contribution. From the EXAFS data analysis the average O−ion−O angle values and the angle variances σ_θ^2 were determined to be 176° and 7°^{2}, respectively, for all three ions, while all the bond−bond correlations were found to be zero. Analyses of the MS signals associated with the 12 O−ion−O rectangular configurations revealed average angle values of 91°,

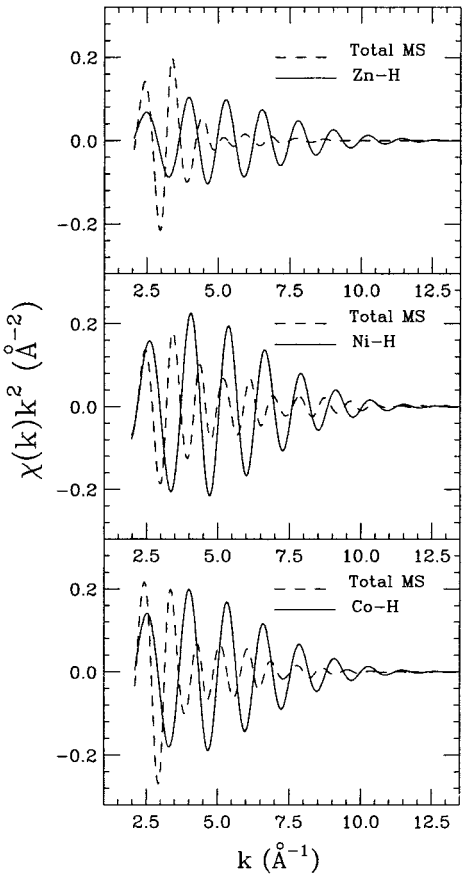

Figure 3. Comparison of the sum of the first shell MS contributions (dashed line) and the ion−H signals (full line) for the Zn^{2+}, Ni^{2+}, and Co^{2+} water solutions (upper, middle, and lower panel, respectively).

92°, and 90°, for Zn, Ni, and Co, respectively, with σ_θ^2 values equal to $6^{\circ 2}$, $4^{\circ 2}$, and $5^{\circ 2}$, respectively. Also in this case bond−bond and bond−angle correlations have been found to be negligible. Figure 3 compares the ion−H signals and the sum of the O−ion−O MS contributions. The amplitude of the ion−H signals is similar to that of the total MS contributions in the region below 4 $Å^{-1}$, while it is much stronger for higher k values. According to these results, a quantitative analysis of the EXAFS spectra of 3d transition metal ions in water can be performed only if both the MS and hydrogen contributions are accounted for.

3.1. First Hydration Shell: The Oxygen Contribution. Several X-ray diffraction (XRD) and neutron diffraction (ND) experiments have been dedicated to the determination of the coordination properties of ionic aqueous solutions.[2] An important advantage of neutron diffraction over X-ray diffraction is the application of the isotopic substitution method (NDIS), which compares experimental data of samples with the same atomic composition, but different isotopes for a particular element. Unfortunately, a rather limited number of isotopes are suitable for NDIS measurements, as isotopes should have reasonably large differences in their scattering lengths. A peculiar and important characteristic of the ND technique is the ability to determine the ion−H (or ion−D) mean distance. Provided the ion−O distance is known, the orientation distribution of the hydrated water molecules can be obtained by neutron diffraction.

The temperature factor information (Debye−Waller factor) obtained from both diffraction and EXAFS data on liquid systems refers to the average of the square of the fluctuations of the distances between the central atom and the scatterer. Therefore, a comparison of the Debye−Waller factors obtained from different techniques can be useful to assess the reliability of the structural results obtained.

From our analysis the short-range hydration structure of Zn^{2+}, Ni^{2+}, and Co^{2+} has been determined with high accuracy. All three ions have been found to be coordinated by six water molecules, in agreement with previous experimental results. Even if for solutions the accuracy of coordination numbers obtained by EXAFS has often been considered low, the existence of octahedral shells has been deduced from the fitting procedures and, in contrast to the methods followed in the analysis of XRD data, a coordination number of six has not been assumed "a priori".

As far as the Zn^{2+} ion is concerned, least-squares refinement of the Zn−O first hydration shell resulted in a bond length of 2.078 Å, with $\sigma^2 = 0.0087$ $Å^2$. The hydration structure of this ion has been thoroughly investigated by XRD and ND and the Zn−O distance varies from 2.08 to 2.10 Å, in good agreement with our result.[2,9] Also the mean square deviation is consistent with the Debye−Waller factors previously determined (0.003−0.03 $Å^2$).[9] It is interesting to outline that the Zn^{2+} first hydration shell parameters obtained by the present analysis are equal, within the reported errors, to those determined by the most recent EXAFS investigation present in the literature.[9]

Among the ions examined in this paper, Ni^{2+} is the one whose hydration structure has been investigated most extensively by XRD, ND, and EXAFS.[2,3,37−40] Moreover, nickel has several stable isotopes, each possessing widely different coherent neutron scattering lengths, and several NDIS studies on Ni^{2+} aqueous solutions have been carried out during the past few years. The distance between the water oxygens in the first hydration shell and the Ni^{2+} ion, as determined in our investigation (2.072 Å), is very close to the value determined by the most recent ND experiment (2.06 Å)[37] and by XRD measurements $(2.05-2.12\ Å)^2$. The value of $\sigma^2 = 0.0046$ $Å^2$ for the first oxygen shell is consistent with the related parameter measured in ND.[3] The most recent EXAFS investigation for a 0.4 molal water solution concluded that six water molecules are located around the Ni^{2+} ion at 2.062(4) Å with $\sigma^2 = 0.0059$-(7) $Å^2$, again in agreement with our determination.[40]

There have been a limited number of structural investigations into Co^{2+} aqueous solutions when compared to those on Ni^{2+} and Zn^{2+}. Moreover, this species is monoisotopic and the aqua ion structure of Co^{2+} is therefore not accessible from NDIS. The best fit analysis of the Co^{2+} water solution EXAFS spectrum performed in the present work suggests a Co−O distance of 2.092 Å, with $\sigma^2 = 0.0062$ $Å^2$. These values are consistent with previous XRD studies $(2.08-2.12\ Å)^2$.

It is interesting to compare the first hydration shell distances obtained for the three ions. The Ni−O bond length is the shortest, while the Co−O one is the largest. The trend in the ion−O bond length variation is consistent with the positions of the minima of the ion−water energy curves obtained from the "ab initio" calculations shown in Figure 5 of ref 23. A different trend has been observed in the case of the mean-square variation

(37) Neilson, G. W.; Ansell, S.; Wilson, J. *Z. Naturforsch.* **1994**, *50a*, 247.
(38) Howell, I.; Neilson, G. W. *J. Mol. Liquids* **1997**, *73, 74*, 337.
(39) Enderby, J. E. *Chem. Soc. Rev.* **1995**, *24*, 159.
(40) Wallen, S. L.; Palmer, B. J.; Fulton, J. L. *J. Chem. Phys.* **1998**, *108*, 4039.

factors σ^2. In particular, the Ni^{2+} water solution shows the highest σ^2 value for the first hydration shell, while the lowest one has been observed for Zn^{2+}. Differences in the Zn^{2+}, Ni^{2+}, and Co^{2+} inner shell coordination σ^2 values have previously been found by Miyanaga et al.,[41] and they were correlated with the ligand water exchange reaction rate and in particular with the strength and stiffness of the ion−O first shell bond. For stable aqua complexes, the residence time of water molecules in the first hydration shell is large and consequently the σ^2 values are expected to be small. It is well established that the hydration structure of Ni^{2+} is quite robust, with long residence time in the first hydration shell, whereas Zn^{2+} has lower kinetic stability. Very little information can be found in the literature on the residence time of water molecules in the first coordination shell of Co^{2+} in aqueous solution. The trend of the σ^2 values in Table 3 reflects the kinetic stabilities of the aqua complexes and shows that the stability of the $[Co(H_2O)_6]^{2+}$ species lies between those of the Ni^{2+} and Zn^{2+} aqua complexes. This finding confirms the hypothesis of Miyanaga et al.[41] and the results obtained from "ab initio" calculations in which the minimum of the ion−water energy curves has been found to be lower for Co^{2+} than for Zn^{2+} (see ref 23).

3.2. First Hydration Shell: The Hydrogen Contribution. This is the first EXAFS investigation of 3d transition metal ions in water solutions where the ion-H contribution has been taken into account. The analysis of the EXAFS signals associated with the hydrogen coordination shells has been carried out by applying a fitting procedure that refines the short-range shape of the MD ion-H $g(r)$'s. The MD ion−H structural parameters reported in Table 1 have been optimized by fitting the EXAFS theoretical signal to the experimental data and the refined values are listed in Table 3. All three ions are coordinated by 12 hydrogen atoms, as expected, at about 2.78 Å, the σ^2 values being 0.016, 0.009, 0.010 $Å^2$ for Zn^{2+}, Ni^{2+}, and Co^{2+}, respectively. Note that the σ^2 factors run parallel to those of the ion−O first hydration shell, and that the largest value has been obtained for Zn^{2+}. Also in this case the trend of σ^2 correlates with the rate constants for water exchange and consequently with the residence times of water molecules in the first hydration shell. However, it is important to stress that the residence times of oxygen and hydrogen atoms in the hydration shell are usually different, because a proton can move faster than an oxygen atom to the next water molecule in the second hydration shell through a hydrogen bond.[2] Therefore, the residence time of protons should be shorter than that of oxygen atoms and the σ^2 values of the ion−H signals are expected to be greater. Obviously, the increase in the ion−H bond variance, as compared to the ion−O one, is also associated with the structural disorder due to the "wagging" motions of the water molecules.

Structural determination of the ion−H $g(r)$'s can be obtained by means of ND measurements, while this information is not accessible from the XRD technique. As a consequence, the coordination geometry of hydrogen atoms in the first hydration shell of ionic solution is usually less known. Note that a further insight into the microscopic structure of aqueous solutions can be gained if we know the ion−H $g(r)$, as this is an additional check on the coordination number and the stability of the first hydration shell, and allows the distribution of local geometries to be better described. Only a few investigations dealing with neutron diffraction studies on the Zn−H pair distributions in water solution can be found in the literature. Two different values of the Zn−H distance (2.69 and 2.74 Å) have been obtained from ND experiments, one of which is in fair agreement with our result.[37] Conversely, several neutron diffraction experiments, often performed with use of the isotopic substitution technique, were dedicated to the determination of the Ni−H $g(r)$ in water solutions with a wide range of concentrations.[3,37,38,42] The most recent study shows that the Ni−H distance is 2.67 Å, 0.1 Å shorter than the one determined by our investigation,[38] while there is no information in the literature on Co−H $g(r)$ in aqueous solutions, due to the lack of ND data. As previously mentioned, the knowledge of the ion−H $g(r)$ facilitates a deeper insight into the geometric properties of water solutions. In particular it is possible to obtain information on the tilt angle ϕ of hydrated water molecules in the first coordination sphere. An early ND study of solutions of $NiCl_2$ in D_2O showed that the tilt angle in the first hydration shell was around 40° in a 4.4 molal solution, and decreased to zero as the concentration was lowered to 0.42 molal.[43] In a more recent investigation, Powell and Neilson[42] indicated that the mean value of the tilt angle calculated on the basis of the Ni−O, Ni−H, and O−H mean distances is misleading. This is because the water molecules in the hydration shell undergo significant "wagging" motions and the probability density of the tilt angle is a more significant quantity. In this work it was concluded that the orientation of water molecules in the Ni^{2+} hydration shell is invariant in the concentration range 0.1 to 2.0 molal and the probability density is quite broad but centered around $\phi = 0$ in a so-called "dipole" type configuration. These contradictory results show that the precise description of the orientation of water molecules around ions in solution is a very difficult task and the existence of an additional experimental technique capable of providing information on the ion−H $g(r)$ is extremely useful. Table 3 shows that the ion−H distances obtained from our analyses are longer than those obtained by ND measurements. This result is consistent with the existence of probability densities centered around $\phi = 0$ for all three ions. The orientation of water molecules in the first hydration shell has also been investigated in terms of probability density, by means of MD simulations, and the results are described in ref 23. These calculations show that in Zn^{2+}, Ni^{2+}, and Co^{2+} water solutions the mean ion−O−H angles are close to 128° and the ion, oxygen, and two hydrogen atoms in a hydrated water molecule lay in one plane in a "dipole" configuration. These findings are consistent with the ion−H distances determined from the present EXAFS data analysis.

In the final step of the analysis, proof of the importance of the hydrogen contributions was obtained by performing additional fitting procedures which did not include the hydrogen signals. The fitting procedures were applied both to the structural parameters associated with the ion−O SS and MS signals and to the nonstructural and background parameters. It is important to outline that the E_0, S_0^2, and the double-electron excitation parameters obtained from these minimizations were equal,

(41) Miyanaga, T.; Sakane, H.; Watanabe, I. *Bull. Chem. Soc. Jpn.* **1995**, *68*, 819.
(42) Powell, D. H.; Neilson, G. W. *J. Phys.: Condens Matter* **1990**, *2*, 3871.
(43) Neilson, G. W.; Enderby, J. E. *J. Phys. C: Solid State Phys.* **1978**, *11*, L625.

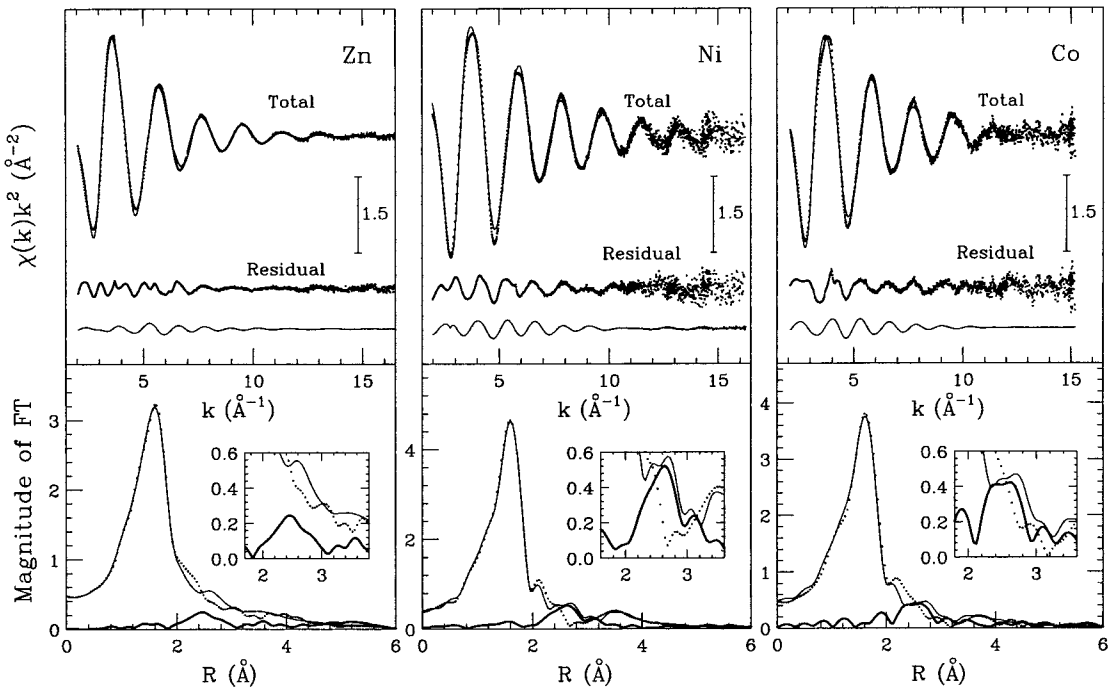

Figure 4. Upper panels: comparisons between the EXAFS experimental spectra of Zn^{2+}, Ni^{2+}, and Co^{2+} in water solutions (left, middle, and right, respectively) and the theoretical signals not including the hydrogen contributions. The last two signals of each panel are the resulting residual curves and the difference between these curves and the residual curves of Figure 2. Lower panels: nonphase-shift-corrected Fourier transforms of the experimental data (dotted line), of the theoretical signals (full line) not including the ion−H signals, and of the residual curves (thick full line). A zoom of the region between 1.8 and 3.6 Å is shown in the insets.

within the reported errors, to those determined from the previous analysis, including the hydrogen contributions. The results of these minimizations are shown in the upper panels of Figure 4, where the total theoretical signals, including the ion−O first and second shells and the MS contributions, are compared with the experimental spectra. In all cases the agreement between the experimental and theoretical signals is not particularly good, especially in the k region below 9 Å^{-1}, and the R_i values were 0.103×10^{-7}, 0.446×10^{-7}, and 0.318×10^{-7} for Zn, Ni, and Co, respectively. The presence of an additional contribution that has not been included in the theoretical calculations is confirmed by looking at the residual curves shown in the upper panels of Figure 4. The amplitude of these signals is quite large and, together with the noise of the experimental spectra, the presence of a leading frequency can be identified clearly. To better characterize this frequency it can be useful to remove the contribution associated with the noise of the experimental data and with the presence of systematic errors in the theory. To this end, the residual curves of Figure 2 have been subtracted from the residuals of Figure 4 and the resulting signals are the last curves shown in the upper panels of Figure 4. These noise-free residuals contain components similar to the ion−H contributions, even if some distortions are visible in the low-k regions. As an aid to assessing the similarity between the theoretical ion−H contributions and the residual signals, comparative plots are shown in Figure 5. Note that both the frequency and the amplitudes of the two curves are in good agreement for all three ions. These results clearly demonstrate that the hydrogen atoms provide a detectable contribution to the XAFS spectra of transition metal aqueous solutions, which has to be accounted for to perform a complete analysis of the experimental data. It is interesting to observe the effect of the omission of the hydrogen contribution on the refined values of

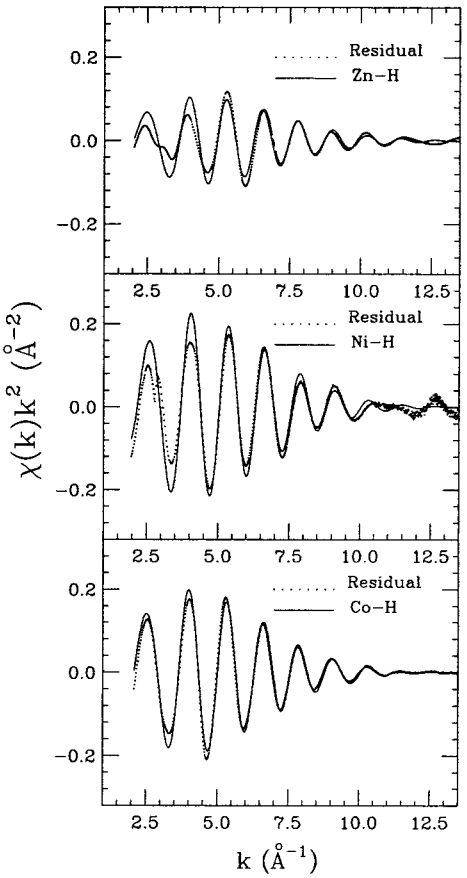

Figure 5. Comparison of the ion−H theoretical signals and the noise-free residual curves of fitting procedures not including the hydrogen contributions.

the structural parameters. All the ion−O first shell parameters determined from the minimization not including the H signals

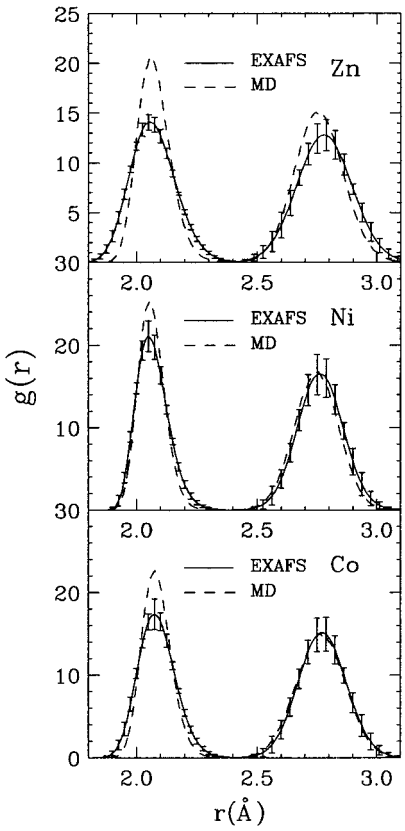

Figure 6. Ion−O and ion−H asymmetric peaks of Zn^{2+}, Ni^{2+}, and Co^{2+} in water (upper, middle, and lower panel, respectively) compared with the MD $g(r)$'s. Error bars on the asymmetric peaks have been computed starting from the statistical erros on individual parameters of Table 3.

were found equal to those of Table 1, within the reported errors. This finding shows that reliable structural information on the ion−H $g(r)$'s can be obtained from the XAS technique, but the exclusion of the hydrogen contribution does not significatively affect the accuracy of the ion−O first shell structural parameters obtained from the EXAFS data analysis. The FT's of the theoretical, experimental, and residual signals of Figure 4 are shown in the lower panels of the same figure. They have been calculated in the same k ranges as the previous analyses, with no phase shift corrections applied. For all three ions the agreement between the theoretical and experimental curves is not very good in the distance range between 2 and 3 Å. The peaks at about 2.5 Å in the FT's of the residual curves, which are better visible in the magnified sections of the FT's of Figure 4, are clearly associated with the hydrogen shell distribution, as no other structural contributions are present in this distance range. It is important to stress that similar discrepancies between theoretical and experimental FT spectra of transition metal ions in aqueous solutions have been observed in previous EXAFS investigations that do not account for the hydrogen contribution.[8,9,40]

3.3. Comparison of EXAFS and MD Results. The refined Zn−O and Zn−H pair distribution functions obtained from the EXAFS data analysis are shown in the first panel of Figure 6 and compared with the results of MD simulations. The Zn−O first peak distances obtained from the two methods coincide within the reported errors[44] (see Tables 1 and 3) but the EXAFS Zn−O first neighbor peak is found to be less asymmetric than predicted by MD. Note that the error bars shown in Figure 6 are based solely on the statistical evaluation, as mentioned above, and they do not include any possible systematic error. The most evident effect is the remarkable difference between the EXAFS and MD Zn−O variance values. As far as the Zn−H $g(r)$ is concerned, the shape of the MD distribution is reproduced by the EXAFS determination, although a shift of about 0.02 Å toward larger distances is found. The comparison between the MD and EXAFS refined $g(r)$ distributions of Ni^{2+} and Co^{2+} is shown in the second and third panels of Figure 6, respectively. In both cases the ion−O and ion−H MD $g(r)$'s are inside the estimated EXAFS error bar, confirming the quality of the potential functions and computer simulation procedures.

A general remark should be made regarding the difference between the EXAFS and the MD σ values of the Zn−O first peak distribution. Similar results were obtained by Kuzmin et al.,[9] and this discrepancy was attributed to the Lennard-Jones potentials used to describe the Zn^{2+}−O interaction. According to our opinion this effect is due, at least in part, to the approximations of the SPC/E water model used in the MD calculations. Moreover, no water molecules in the first hydration shell exchanged with the bulk during the nanosecond of simulation. Therefore, the effect of the kinetic stability of the aqua complexes on the variance of the $g(r)$ distributions is not reproduced by the MD simulations. Note that the best agreement between the MD and EXAFS results has been obtained for Ni^{2+}, which possesses the most stable hydration sphere and the largest residence time of water molecules in the first coordination shell.

3.4. Second Hydration Shell. The last remark we would like to make concerns the possibility of using the EXAFS technique to gain structural information on the second coordination shell of transition metal ions in water solutions. As outlined above the second hydration shell contributions to the XAFS spectra have been calculated directly from the tails of the MD ion−O $g(r)$'s and they have been kept fixed during the minimization. This procedure enables the calculation of the effective contribution of the second hydration shell distribution as derived from MD calculations. In particular, our MD simulations suggest the presence of second shells formed by about 13 water molecules at about 4.27 Å with $\sigma^2 = 0.12$ Å^2 (see Table 1). The coordination numbers and the mean square deviations agree well with the average values provided by XRD and ND studies,[2] reinforcing the reliability of the MD $g(r)$'s. Figure 2 shows that the amplitude of the second shell signals is below the experimental noise of the spectra and that it is much lower than both the ion−H and MS contributions. This finding is not surprising as the second shell is quite broad and occurs at distances longer than 4 Å. This gives rise to a damped signal that could be observed only in the k-range below 1.5 Å^{-1}.

From these results it is clear that the EXAFS technique is not suitable for determining the structure of the second hydration shells of Zn^{2+}, Ni^{2+}, and Co^{2+} in water solutions. As mentioned, the suitability of the EXAFS technique for obtaining structural information beyond the first hydration shell of ionic solutions has been hotly debated. To explain the structure around 3d metal cations in aqueous solutions, some authors have argued that the small peak appearing in the FT at about 4 Å is partially or totally due to the second hydration shell.[8−10] In particular, the question of the contribution of the second hydration shell to the XAFS

(44) Di Cicco, A. *Phys. Rev. B* **1996**, *53*, 6174.

spectra of Zn^{2+} aqueous solutions has been raised in two previous works. In one of the papers[8] the authors attributed the high-frequency signal of the EXAFS spectra to a second hydration shell composed of 11.6 ± 1.6 water molecules located at 4.1 ± 0.2 Å, with $\sigma^2 = 0.039 \pm 0.009$ Å^2. In that investigation no MS calculations have been carried out, and the second shell structural parameters derived from the EXAFS analysis are quite different from those provided by XRD.[2] In particular the second shell distance is too short and the mean square deviation is too small. In the other paper[9] no evidence of significant contributions from the second hydration shell was found in the EXAFS spectra of Zn^{2+} aqueous solution. The authors explained this in terms of the cancellation interference effect between the Zn−O second shell and the $Zn-O_{1^{st}\,shell}-O_{2^{nd}\,shell}$ MS contributions in the presence of strong thermal and structural disorder. However, these SS and MS signals have been found to give a detectable contribution only in the k region below 4 Å^{-1} and their amplitudes are less than 2% of the total $\chi(k)$ structural signal and thus in agreement with our results.

4. Conclusions

A detailed investigation of Zn^{2+}, Ni^{2+}, and Co^{2+} water solutions has been carried out combining MD simulations with EXAFS experimental data. The ion−O first shell structural parameters have been accurately determined and the short-range sensitivity of the EXAFS technique has been used to test the reliability of the potential functions used in the MD simulations.

A thorough insight into the interpretation of the high-frequency component of the EXAFS spectra of 3d transition metal ions in water solution has been obtained with the aid of long-range structural information derived from MD calculations. The high-frequency contribution present in the EXAFS spectra has been found to be due to MS effects inside the ion−O first coordination shell.

The MD simulations showed the existence of well-defined second hydration shells, whose contribution to the EXAFS spectra has been found to be negligible. These results demonstrate that no information on the well-established second sphere of water molecules surrounding the Zn^{2+}, Ni^{2+}, and Co^{2+} ions can be obtained by the EXAFS technique. On the other hand, it has been shown that the inclusion of the hydrogen contribution is essential to perform a quantitative analysis of the studied systems. The EXAFS technique has been proven to provide reliable structural information on the ion−H pair distribution functions of ionic solutions, which can be difficult or impossible to obtain by other experimental techniques.

The results of the present investigation represent a step forward in the correct EXAFS analysis of transition metal ionic solutions and may stimulate further investigations into the role of hydrogen atoms in EXAFS spectra of aqueous systems.

Acknowledgment. We thank the European Union for support of the work at EMBL Hamburg through the HCMP Access to a Large Installation Project, Contract No. HPRI-CT-1999-00017, and the CASPUR computational center for providing the computer architectures used in this work. Paola D'Angelo was supported by an institutional EU fellowship, Contract No. ERBCHBGCT930485. This work was sponsored by the Italian National Research Council and by the Italian Ministry for the University and the Scientific and Technological Research (MURST).

JA015685X